Chapter 1

Constructing C^1 surfaces of arbitrary topology using biquadratic and bicubic splines

Jörg Peters

1.1. Introduction

Two approaches to building smooth free-form surfaces, generalized subdivision and the composition of surfaces from patches, are combined to generalize biquadratic tensor-product B-splines surfaces. The result is a low degree polynomial surface representation with control via the input mesh of points. The simplicity of the construction forces the surface to closely follow the design intent expressed by the input data.

Cutting corners and edges to smooth a polytope is a geometrically intuitive design paradigm. Algorithmically, it is realized by generalized subdivision. Given an input mesh of points delineating a surface, the algorithms of [4], [6], [14], [8] etc. create at each stage a refined mesh of points by averaging neighboring points of the current mesh. Where the mesh is *regular*, e.g. where each mesh point is surrounded by exactly four quadrilateral cells, the mesh points can be interpreted as B-spline control points and the refinement of the mesh as the subdivision of the spline. Thus the limit surface has a standard parametrization of low degree. Unfortunately, regular meshes can only model very restricted geometric configurations. Modeling real world objects without singularity and such that the mesh conforms with the features, generally requires an irregular mesh and, for such meshes, generalized subdivision methods do not provide an explicit parametrization of the limit surface. This not only makes it tricky to establish elementary properties like tangent plane continuity of the limit surface (see e.g. [7], [1],[2],[3]), but is also a major obstacle for integrating these techniques with other computer aided design representations.

Assembling surfaces from patches is a second design paradigm. A number of surface constructions for irregular meshes have been derived over the last decade [10]. Compared to the standard tensor product B-spline representation, these constructions either sacrifice the low degree of the surfaces (e.g. [20],[12]) or depart from the standard polynomial representation (e.g. [5], [16]). However,

the main drawback of the patching approach seems to arise from the very tool that allows it to model complex smooth surfaces; reparametrizing when crossing from one patch to the next shifts the focus from the geometry of the modeling problem to clever uses of the chain rule. Thus the algorithms of [9], [13] and [17] fix the reparametrizations *a priori* depending only on the number of the patches joining at a mesh point; in order to match geometric data, a large sparse linear system is solved. This makes it tricky to reason about the shape of the resulting surface.

The algorithm proposed here reconciles the subdivision paradigm with the parametric approach. It generalizes the standard biquadratic tensor-product spline representation to irregular meshes. In particular, there are no regularity restrictions on the input mesh as in [21]. The underlying idea is to use a small number of subdivisions to give the surface its rough shape and separate irregular mesh regions. Then a biquadratic C^1 spline can be fit over the regular mesh regions and the remaining mesh holes can be covered by a composite of bicubic patches. The result is a polynomial surface of low degree. Since no system of equations has to be solved to determine the parametrization, but rather the input mesh points are averaged such that de Casteljau's algorithm generates a C^1 surface in the limit, the method is a generalized subdivision algorithm. Additionally, one can interpolate the vertices of the input mesh and normals at the vertices without solving systems of equations.

The structure of the article is as follows. Section 2 states the algorithm. Section 3 establishes the consistency and continuity of the resulting surfaces and proves simple shape properties. Section 4 gives examples and Section 5 summarizes the findings.

1.2. The Algorithm

The three steps of the algorithm are:

- Refining the input mesh to isolate irregular mesh points by regular B-spline control points.
- (Optional) Converting the quadratic B-spline surface into Bernstein-Bézier form to make the representation uniform.
- Covering the irregular mesh cells with bicubic patches.

The *input* is any mesh of points such that at most two cells abut along any edge. The mesh cells need not be planar, and there is no constraint on the number of edges to a cell or the number of cells meeting at a vertex. The mesh may model a bivariate open or closed surface of arbitrary topological structure. Each cell f of the input mesh has a shape parameter α_f, called *blend ratio*. The blend ratio is a number between zero and one. A smaller ratio results in a surface that follows the input mesh more closely and changes the normal direction more rapidly close to the mesh edges. The *output* of the algorithm are the Bernstein-Bézier coefficients of biquadratic and bicubic patches that parametrize a tangent-plane continuous surface. The surface interpolates the centroid, the average of the vertices, of each cell of the input mesh.

The end of this section gives two simple extensions of the algorithm that guarantee interpolation of the mesh vertices and allow for a rational surface representation.

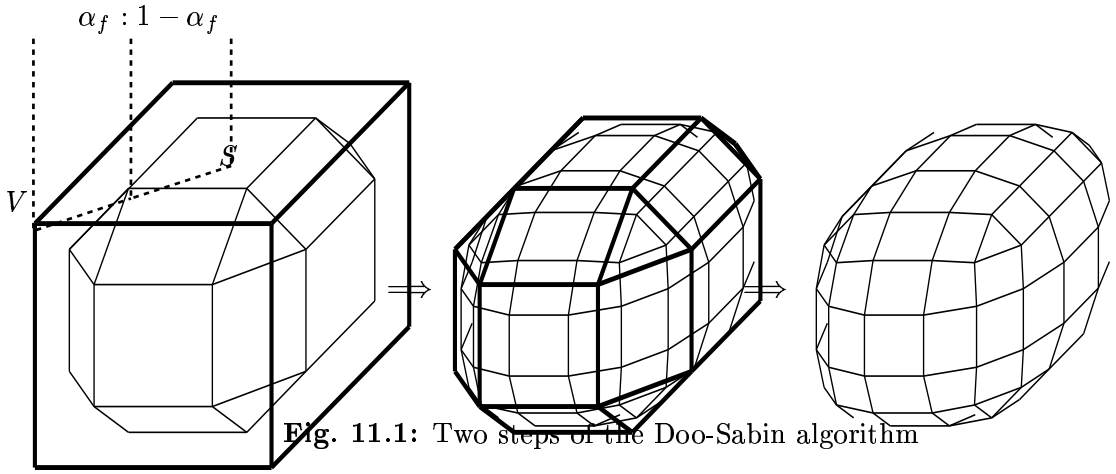

Fig. 11.1: Two steps of the Doo-Sabin algorithm

A1. Refining the input mesh to separate irregular mesh points by layers ofregular B-spline control points.

The refinement gives the object its rough shape and isolates non quadrilateral mesh cells. It consists of two steps of Doo and Sabin's averaging procedure [6]. At each step, s new points are created for each s-sided cell. Each new point connects to four new points, two generated at the two adjacent vertices of the same cell and two corresponding to adjacent cells of the same old mesh point cf. Fig. 11.1. A new point corresponding to a vertex V of the cell f with centroid S and n edges has the coordinates $(1-\alpha_f)V + \alpha_f S$ in the first step and

$$(1-\alpha)V + \alpha S, \quad \alpha := \alpha_f(1-\cos(2\pi/n))$$

in the second step.

After refining the mesh, each mesh point is surrounded by four cells. If, the mesh point is *regular*, that is, if all four cells have exactly four edges, then the nine mesh points defining the cells can be interpreted as the control mesh of a quadratic spline. To guarantee a C^1 construction also at the irregular mesh points, the refined mesh has to be perturbed in some cases. Let $B_{i,j}$ be the mesh points edge-adjacent to the vertex C_i of an n-sided cell of the refined mesh (cf. Figure 1.2.2) and define

$$E := \frac{-1}{2n}\sum_{i=1}^{s}\sum_{j=1}^{2}(-1)^{i+j}B_{i,j}.$$

If n is even and greater than four, then the $B_{i,j}$ are replaced by $B_{i,j}+(-1)^{i+j}E$.

If $\alpha_f = 1/2$ uniformly, the cells of the refined quadrilateral mesh correspond to the same quadratic and can be stored more efficiently [6, p 163]. If the input

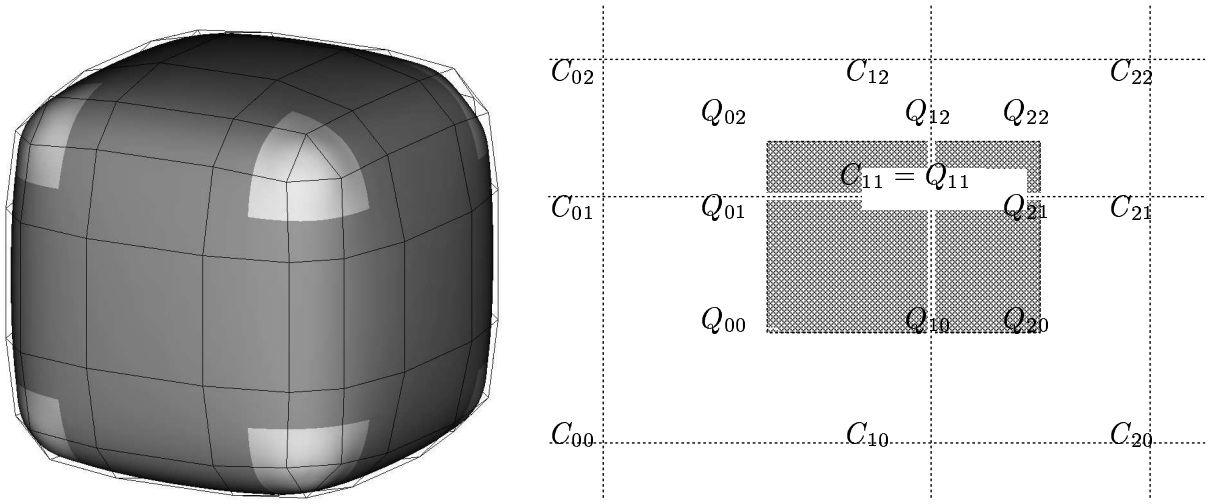

Figure 1.2.1: *Darker regions are parametrized by biquadratics.*

mesh already satisfies some or all conditions R1–R3 of Proposition 1.3.1, then only one or no refinement step is necessary.

A2. (Optional) Converting the biquadratic B-spline surface into Bernstein-Bézier form

Any submesh of regular points of the refined mesh can serve as the control mesh of a biquadratic tensor product spline surface. The spline be expressed in Bernstein-Bézier form in order to unify the representation with the representation at the irregular mesh sites. By symmetry, it suffices to give the conversion formulae for the following four Bernstein-Bézier coefficients Q_{ij} in terms of the spline control points C_k (cf. Figure 1.2.1)

$$\begin{aligned} Q_{00} &= (C_{00} + C_{10} + C_{01} + C_{11})/4, \\ Q_{10} &= (C_{11} + C_{10})/2, \\ Q_{01} &= (C_{11} + C_{01})/2, \text{ and} \\ Q_{11} &= C_{11}. \end{aligned}$$

As a second example, the mesh cell $A_iB_{i,1}C_iB_{i,2}$ in Figure 1.2.2 yields $L_i = Q_{00} = (A_i + B_{i,1} + C_i + B_{i,2})/4$, $Q_{01} = (C_i + B_{i,2})/2$ and $Q_{11} = B_{i,2}$ for the coefficients Q_{ab} of $q_{i,2}$.

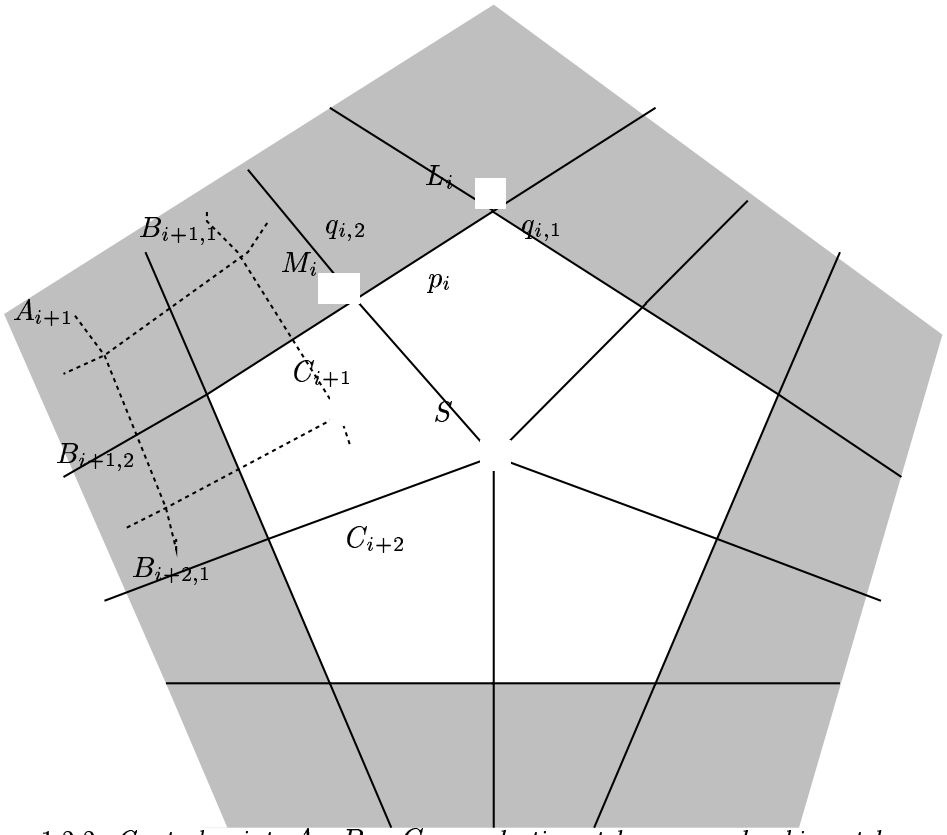

Figure 1.2.2: *Control points A_i, B_{ij}, C_i, quadratic patches q_{ij} and cubic patches p_i.*

A3. Covering the irregular mesh cells with bicubic patches.

The refinement step and the interpretation of the regular mesh points of the refined mesh as B-spline control points creates a parametrically C^1 biquadratic tensor-product surface with non quadrilateral holes. Each hole is split into quadrilaterals as indicated in Figure 1.2.2. Each quadrilateral is covered by a bicubic patch. The ith patch, p_i, has coefficients $P_{kl,i}$, $k,l = 0..3$ such that $P_{00,i}$ corresponds to the corner point L_i of the biquadratic surface and $P_{33,i}$ corresponds to the central point S where the bicubic patches join.

To join the bicubic patch smoothly to the biquadratic surface, the boundary curves are the degree-raised quadratics:

$$P_{00,i} = \frac{1}{4}(B_{i,2} + B_{i,1} + C_i + A_i), \quad P_{20,i} = \frac{1}{12}(5B_{i,2} + B_{i+1,1} + 5C_i + C_{i+1}),$$
$$P_{10,i} = \frac{1}{12}(5B_{i,2} + B_{i,1} + 5C_i + A_i), \quad P_{30,i} = \frac{1}{4}(B_{i,2} + B_{i+1,1} + C_i + C_{i+1}),$$

and the coefficients defining the transversal derivatives are chosen as

$$\begin{aligned}
P_{11,i} &= \frac{1}{36}(5B_{i,2} + 5B_{i,1} + A_i + 25C_i) + \frac{a}{9}(C_i - A_i) \\
P_{21,i} &= \frac{1}{36}(5B_{i,2} + 5C_{i+1} + B_{i+1,1} + 25C_i) \\
&\quad + \frac{a}{18}(-5B_{i,2} + B_{i+1,1} + C_{i+1} + 3C_i) \\
P_{31,i} &= \frac{1}{12}(B_{i,2} + B_{i+1,1} + 5C_{i+1} + 5C_i) + \frac{a}{6}(C_{i+1} + C_i - B_{i,2} - B_{i+1,1})
\end{aligned}$$

where $a := \frac{c}{1-c}$ and $c := \cos(\frac{2\pi}{n})$. The coefficients $P_{0k,i}$ and $P_{1k,i}$, $k = 0..3$ are obtained by symmetry. For example, $P_{12,i} = \frac{1}{36}(5B_{i,1} + 5C_{i-1} + B_{i-1,2} + 25C_i) + \frac{a}{36}(-11B_{i,1} + 3B_{i-1,2} + 3C_{i-1} + 5C_i)$. The definition of the surface is completed by setting

$$\begin{aligned}
P_{33,i} &= S = \frac{1}{n}\sum_{i=1}^{n} C_i \\
P_{32,i} &= P_{23,i+1} = S + \frac{4\alpha}{3n}\sum_{l=1}^{n} \cos(\frac{2\pi}{n}l) P_{31,i+l}, \\
P_{22,i} &= \begin{cases} -\sum_{j=1}^{n}(-1)^j E_{i+j} & \text{if } n \text{ is odd} \\ \frac{-2}{n}\sum_{j=1}^{n}(n-j)(-1)^j E_{i+j} & \text{if } n \text{ is even.} \end{cases}
\end{aligned}$$

The scalar $\alpha \in [0,1]$ is a shape parameter proportional to the diameter of the tangent plane of first differences (cf. [15, Fig.3]) and therefore similar to the blend ratio of the Doo-Sabin algorithm. Its default setting is $\alpha = 1$. The vector

$$E_i := (1 - \frac{2c}{3})P_{32,i} + \frac{2c}{3}P_{31,i}$$

is an average of the interior coefficients of the boundary curve.

1.2.1. Extensions of the algorithm.

A1a. Interpolation at the vertices of the input mesh. After the first of two refinements in Step A1, move the control points C_i, $i = 1..n$ whose construction involves S by $S - \frac{1}{n}\sum_{i=1}^{n} C_i$ for each vertex S of the input mesh. Then S is the centroid of the resulting cell and will be interpolated. Similarly, one can interpolate normals at the vertices.

A2a. Conic blends and rational patches. To obtain conic blends and, more generally, rational surfaces, treat the control points as vectors in $\mathbb{R}^4$ and the fourth coordinate as an additional shape parameter. If $P, Q : [0,1]^2 \mapsto \mathbb{R}^3$ and $p, q : [0,1]^2 \mapsto \mathbb{R}$ and $P = Q$ and $p = q$ along a boundary shared by the functions P/p and Q/q, then the continuity conditions (see next page)

$$D_1(\frac{Q}{q} \circ \phi) = D_1 \frac{P}{p} \qquad \Longleftrightarrow$$

$$q(D_1P - D_1QD_1\phi^{[1]} - D_2QD_1\phi^{[2]}) = Q(D_1p - D_1qD_1\phi^{[1]} - D_2qD_1\phi^{[2]})$$

hold along that boundary if the masks of the algorithm are applied to the coefficients of $(P, p) \in \mathbb{R}^4$. That is, the fourth coordinate corresponds to the rational weight function. For example, choosing the weight component of two neighboring control points in the regular mesh to be 3 rather than 1 (and keeping the other weight components at 1) yields two circular arcs with weights (112) and one conic with weights (232) in between:

weights of the control points	1		1		3		1	1
weights of three quadratic boundary curves		1	1	2	3	2	1	1
weights of the control points	1		1		3		1	1

In general, the algorithm works for constructing bivariate surfaces in $\mathbb{R}^n$.

A3a. An alternative choice of the tangent plane at S. By default, the tangent coefficients $P_{32,i}$ at S should be constructed symmetrically from the existing data. Since the tangent coefficients P_{31} at M are constructed by applying a mask to the control points, B_{ij} and C_i, one can simplify the formulae by making $P_{32,i}$ depend only on the C_i and ignoring the contribution of the B_{ij}.

$$P_{32,i} = S + \frac{4\alpha}{3n}\sum_{l=1}^{n} \cos(\frac{2\pi}{n}l)\frac{C_{i+l} + C_{i+1+l}}{2}.$$

1.3. Structure, smoothness and shape of the surface

This section analyzes the construction. The first part examines the refinement process. The second proves consistency and smoothness of the surface. The third discusses shape properties of the resulting surface. The fourth considers the special case of triangular mesh cells.

1.3.1. Mesh structure.

Denote as c-c every pair of non-4-sided cells arising from two adjacent non-4-sided cells or from two adjacent non-4-valent vertices and as v-c every pair of non-4-sided cells arising from a non-4-sided cell and its non-4-valent vertex.

PROPOSITION 1.3.1 *The two refinements in Step* A1 *result in a mesh such that* R1 *every interior control point has four neighbors,* R2 *every* c-c *pair is separated by three layers of quadrilateral cells and* R3 *every* v-c *pair is separated by one layer of quadrilateral cells.*

Proof. Since every new control point is connected to two new points on the same original cell and across to edges of that cell, R1 holds already after the first step. One step separates any two cells by one layer of quadrilateral cells. This implies R2. R3 follows from the same argument since every v-c pair still has a common vertex after the first refinement.

COROLLARY 1.3.2 *The control points $B_{i,j}$ of a* v-c *pair of cells are distinct. The perturbation of any $B_{i,j}$ does not alter the control points of a cell that contains the centroid of a cell of the input mesh.*

Since the endpoints of the new and old edges together with the centroid form similar triangles, the refinement leaves all facet-cell edges parallel to the original facet cells.

1.3.2. Smoothness.

This section shows that splines generated by the surface form a smooth vector space. Here smoothness stands for oriented tangent plane continuity which is characterized as the agreement of the derivatives of two maps p and q from $\mathbb{R}^2$ to $\mathbb{R}^n$ after reparametrization by a map φ from $\mathbb{R}^2$ to $\mathbb{R}^2$ that connects the domains Ω_p and Ω_q of p and q:

$$p = q \circ \varphi \quad \text{and} \quad D_1 p = D_1(q \circ \varphi) \quad \text{along } E_p$$

where $\varphi(E_p) = E_q$, E_p and E_q are edges of Ω_p and Ω_q respectively. D_1 denotes differentiation in the direction perpendicular to E_p and the connecting map φ maps interior points of Ω_q to exterior points of Ω_p thus avoiding cusps. The components of φ are $\varphi^{[1]}$ and $\varphi^{[2]}$

THEOREM 1.3.3 *The surfaces generated by the algorithm are tangent plane continuous. Surfaces generated from input meshes with the same connectivity and the same blend ratio for corresponding cells form a smooth vector space.*

The proof of the first part of the theorem is divided into four lemmas.

The first proves smoothness between the biquadratic patches, the second and third between biquadratics and bicubics at L_i and M_i and the fourth between bicubics at S (cf. Figure 1.2.2). Showing that the cubic polynomials $D_1(p_i - q_{i,j} \circ \phi_{ij})$ and $D_1(p_{i-1} - p_i \circ \psi_i)$ and their D_2 derivatives vanish at L_i, M_i and S implies that they vanish identically establishing overall smoothness. The vector space property follows from the linearity of the algorithm for fixed blend ratios and connecting maps and the observation that two surfaces generated from input meshes with the same connectivity have a natural correspondence of abutting patches and hence are joined by the same connecting map.

LEMMA 1.3.4 *The conversion of the regular mesh points in Step* A2 *generates the Bernstein-Bézier coefficients of a parametrically C^1 surface equivalent to the biquadratic tensor-product spline.*

Proof. Since the centroid of any four points is also the intersection of lines through opposite midpoints, the transversal derivatives across any boundary agree pairwise. That is, $D_1 q_1 = D_1 q_2$ and $\varphi = \mathrm{id}$ for adjacent patches q_1 and q_2 as claimed.

LEMMA 1.3.5 *The extensions of the biquadratic patches $q_{i,1}$ and $q_{i,2}$ define the mixed derivative of p_i at L_i consistently.*

Proof. Choose the coordinate system such that $p_i(0,0) = L_i$ and $p_i(1,0) = M_i$. Then for each patch $q_{i,j}$, $j = 1, 2$, the patch p_i is chosen such that $p_i = q_{i,j} \circ \phi_{i,j}$ and $D_j p_i = D_j(q_{i,j} \circ \phi_{i,j})$ along the common boundary, where $a := \frac{c}{1-c}$, $c := \cos(\frac{2\pi}{n})$ and

$$\phi_{i,1} := \mathrm{id} + t_1 t_2 \begin{bmatrix} a \\ a(1-t_2) \end{bmatrix}, \qquad \phi_{i,2} := \mathrm{id} + t_1 t_2 \begin{bmatrix} a(1-t_1) \\ a \end{bmatrix}.$$

For simplicity, we drop the subscript i and do not explicitly mention that we evaluate at the origin.

We need to show that

$$D_1 D_2(q_1 \circ \phi_1) = D_1 D_2 p = D_1 D_2(q_2 \circ \phi_2). \tag{L}$$

Expanding the left hand side of (L) according to the chain rule and noting that $D_2\phi_1 = (0,1)$ and $D_1\phi_2 = (1,0)$, we have

$$D_1 D_2 q_1 + D_1 q_1 D_1 D_2 \phi_1^{[1]} + D_2 q_1 D_1 D_2 \phi_1^{[2]} = D_1 D_2 q_1 + a_1 D_1 q_1 + a_2 D_2 q_1.$$

The expression for the right hand side is obtained by symmetry. By construction of the complex, $D_1 D_2 q_1 = A + C - B_1 - B_2 = D_1 D_2 q_2$. and $D_j q_2 = D_j q_1$. Thus the left hand side of (L) equals the right hand side and uniqueness of the mixed derivative $D_1 D_2 p$ follows.

LEMMA 1.3.6 *The patches join smoothly at M_i.*

Proof. We choose the coordinate system such that $p_i(0,0) = M_i$ and $p_i(1,0) = L_{i+1}$. Then

$$D_2^m p_i = D_2^m(q_{i,1} \circ \phi'_{i,1}), \quad m = 0,1$$
$$D_2^m p_{i-1} = D_2^m(q_{i-1,2} \circ \phi'_{i-1,2}), \quad m = 0,1$$

along the common boundary, where $a := \frac{c}{1-c}$, $c := \cos(\frac{2\pi}{n})$ and

$$\phi'_{i-1,2}(-t_1, t_2) = \phi'_{i,1}(t_1, t_2) = \mathrm{id} + at_2(1-t_1)\begin{bmatrix} t_1 \\ 1 \end{bmatrix}.$$

We show that this choice of reparametrization is consistent with the smooth join of the bicubic patches

$$D_1^m p_{i-1} = D_1^m(p_i \circ \psi'_i) \quad m = 0,1, \quad \psi'_i := \mathrm{id} + t_1 t_2 \begin{bmatrix} -2c \\ 0 \end{bmatrix}. \tag{M}$$

For simplicity, we do not explicitly mention in the following that we evaluate at the origin. For $m = 0$, we check $p_{i-1} = p_i \circ \psi'_i$, $D_2 p_{i-1} = (1+a)D_2 q_{i-1,2} = (1+a)D_2 q_{i,1} = D_2(p_i \circ \psi'_i)$, and $D_1 p_{i-1} = D_1 q_{i-1,2} = D_1 q_{i,1} = D_1 p_i = D_1(p_i \circ \psi'_i)$. For $m = 1$, we observe that $D_1 D_2 q_{i-1,2} = D_1 D_2 q_{i,1}$, $D_1 q_{i-1,2} = D_1 q_{i,1}$ and hence

$$\begin{aligned} D_2 D_1 p_{i-1} &= D_2 D_1(q_{i-1,2} \circ \phi'_{i-1,2}) \\ &= (1+a) D_1 D_2 q_{i-1,2} + a(D_1 q_{i-1,2} + D_2 q_{i-1,2}) \\ &= D_2 D_1(q_{i,1} \circ \phi'_{i,1}) + 2a D_2 q_{i,1} \\ &= D_2 D_1 p_i + \frac{2a}{1+a} D_2 p_i. \end{aligned}$$

The claim follows since $D_2 D_1(p_i \circ \psi'_i) = D_2 D_1 p_i - 2c D_1 p_i$. and $\frac{2a}{1+a} = -2c$.

LEMMA 1.3.7 *The bicubic patches meet smoothly at S.*

Proof. We choose the coordinate system such that $p_i(0,0) = p_{i-1}(0,0) = S$ and $p_i(1,0) = M_i$ and show that

$$D_1 p_{i-1} = D_1(p_i \circ \psi_i), \quad \text{where} \quad \psi_i := \mathrm{id} + t_1(1-t_2)\begin{bmatrix} 2c \\ 0 \end{bmatrix}. \tag{I}$$

In Bernstein-Bézier form this yields 4 constraints. Since two of these hold at M by the previous Lemma, we need only show that

$$2(1-c)S = P_{32,i-1} - 2cP_{32,i} + P_{32,i+1} \tag{I$_3$}$$
$$2((1-\frac{2c}{3})P_{32,i} + \frac{2c}{3}P_{31,i}) = P_{22,i-1} + P_{22,i} \tag{I$_4$}$$

to establish tangent plane continuity between adjacent bicubics p_i and p_{i-1}. Constraint I_3 holds since

$$\sum_{i=1}^{n} \cos(\frac{2\pi}{n}i)(P_{31,i-1} - 2cP_{31,i} + P_{31,i+1})$$
$$= \sum_{i=1}^{n} P_{31,i}\big(\cos(\frac{2\pi}{n}(i-1)) + \cos(\frac{2\pi}{n}(i+1)) - 2\cos(\frac{2\pi}{n})\cos(\frac{2\pi}{n}i)\big) = 0.$$

If n is odd, then

$$P_{22,i-1} + P_{22,i} = -\sum_{j=1}^{n}(-1)^j(E_{i+j-1} + E_{i+j}) = 2E_i$$

as required by (I_4). If n is even, then

$$\sum_{j=1}^{n}(-1)^j P_{32,j} = \frac{\alpha}{n}\sum_{j=1}^{n}(-1)^j \sum_{l=1}^{n} \cos(\frac{2\pi}{n}l)P_{31,j+l} = 0$$

since $\sum_{j=1}^{n}(-1)^j \cos(\frac{2\pi}{n}j) = 0$ and $\sum_{j=1}^{n}(-1)^j P_{31,j} = 0$ since the C_i cancel and the perturbation forces $E := \sum_{i=1}^{n}\sum_{j=1}^{2}(-1)^{i+j}B_{i,j} = 0$. ($E = 0$ is also a necessary constraint for solvability.) Therefore $\sum_{j=1}^{n}(-1)^j E_j = 0$ and

$$P_{22,i-1} + P_{22,i} = \frac{-2}{n}\sum_{j=1}^{n}(n-j)(-1)^j(E_{i+j-1} + E_{i+j})$$
$$= \frac{-2}{n}\big(\sum_{j=1}^{n}(-1)^j E_j - nE_i\big) = 2E_i$$

as required.

The join between the bicubic patches with the above connecting map leaves three coefficients at S free to choose. Since $E = 0$, it is always possible to solve the least squares problem

$$\min \sum_{i=1}^{s} \|P^*_{32,i} - P_{32,i}\|^2 + \sum_{i=1}^{s} \|P^*_{22,i} - P_{22,i}\|^2$$

subject to the constraints I_3 and I_4, where the $P^*_{32,i}$, $P^*_{22,i}$ are desirable locations obtained, say, from degree-raising. The particular solution used in the algorithm has the advantage of being explicit and symmetric. We also note that if $n = 4$, and hence $a = 0$, then the patches generated by Step A3 are biquadratic rather than bicubic.

1.3.3. Shape considerations.

This section shows that the surface is locally flat exactly when the input mesh is locally flat. It also characterizes monotonicity for symmetric data and proves that the surface tautly interpolates the input mesh when the blend ratios are zero.

PROPOSITION 1.3.8 *A biquadratic patch with center coefficient Q_{11} generated in Step* A2 *has zero curvature if and only if the four cells surrounding the meshpoint $C_{11} = Q_{11}$ are coplanar. Two adjacent coplanar cells, give rise to a linear boundary curve.*

Proof. The 9 by 9 system of equations relating the control points to the Bernstein-Bézier coefficients is of full rank. While the linearity of the boundary curve follows from coplanarity, the reverse does not hold, because the system is 3 by 6.

PROPOSITION 1.3.9 *The curvature at S is zero if and only if $P_{31,i}, i = 1..s$ and S lie in the same plane.*

Proof. According to Lemma 1.3.7, all $P_{32,i}$ and S lie in the same tangent plane. Let $P(n)$ be the component of P normal to that plane. If some $P_{31,i}$ does not lie in that plane, then the curvature of the ith boundary curve is nonzero and the $P_{22,i}$ do not all lie in the plane either. The latter follows by contradiction from I_4: $2cP_{31,i} = 2((1-c)P_{32,i}(n) + cP_{31,i}(n)) = P_{22,i-1}(n) + P_{22,i}(n) = 0$. Conversely, if all $P_{31,i}$ lie in the tangent plane, then the normal components of all $P_{32,i}$ and $P_{22,i}$ are zero by construction.

COROLLARY 1.3.10 *If all C_i and $(B_{i,1}+B_{i,2})/2$ are in the same plane, then the normal curvatures at S are zero. If additionally all A_i and $(B_{i,1} - B_{i,2})/2$ are in the common plane, then the bicubic patch is flat.*

To analyze monotonicity of the surface define the averages $S_P := \frac{1}{s}\sum_{i=1}^{s} P_{31,i}$ and $S_C := \frac{1}{s}\sum_{i=1}^{s} C_i$. Assume *local symmetry* of the control mesh at S i.e. A_{i+1}, $B_{i+1,j}$ and C_{i+1} can be obtained from A_i, B_{ij} and C_i by a rotation by $\frac{2\pi}{n}$ and *local convexity* of the control mesh, i.e. the extensions of the cells spanned by A_i, B_{ij} and C_i $i = 1..s$ form a convex cone. Let $\beta^* \geq 1$ be the smallest value such that $S_C + \beta^*(S_P - S_C)$ intersects the cone. Then we can more generally choose $P_{33,i} = S = S_C + \beta(S_P - S_C)$. Setting $\beta = 0$ guarantees interpolation at the centroid.

LEMMA 1.3.11 *If the control mesh is locally convex and symmetric, then for $s > 4$ the boundary curves are convex if $1 \leq \beta \leq \beta^*$; for $s = 3$, $\beta = 1$ is sufficient. If $s > 4$, then the components $P_{ij}(n)$ of the coefficients normal to the tangent plane are monotonically increasing with $i + j$ if and only if $A(n) > \frac{4+8a}{5a-1}B(n)$.*

Proof. Due to symmetry the C_i are coplanar and we may denote the normal distance of a point P from that plane by $P(n)$. Dropping the subscripts of the control points we have $A(n) < B(n) < C(n) = 0 < \beta = P_{32,i}(n) = S(n)$. By

symmetry, the curve with coefficients $[P_{30,i}, 3P_{31,i}, 3P_{32,i}, P_{33,i}]$ constructed in Step A3 falls into a perpendicular plane. Since $1 < a = \frac{1}{1-c}$ for $s > 4$, and $B(n) < 0$,

$$P_{31,i}(n) = \frac{1-2a}{6} B(n) > 0.$$

That is, the plane through the C_i separates the M_i from the plane in which S and the coefficients $P_{32,i}$ lie if $S = S_C$. The boundary cubic has therefore an inflection in the Bernstein-Bézier polygon unless $\beta \geq 1$, i.e. $S(n) \geq P_{31,i}(n)$.

For $s > 4$, set $A(n) =: kB(n)$, $k > 1$ and $b := \frac{1-2a}{6} < 0$. Since $\beta \geq 1$, $P_{33}(n) = P_{31}(n) + \epsilon b B(n)$, $\epsilon \geq 0$. Then

$$\begin{bmatrix} P_{03} & P_{13} & P_{23} & P_{33} \\ P_{02} & P_{12} & P_{22} & P_{32} \\ P_{01} & P_{11} & P_{21} & P_{31} \\ P_{00} & P_{10} & P_{20} & P_{30} \end{bmatrix} (n)$$

$$= \begin{bmatrix} \frac{1}{2} & b & (1+\epsilon)b & (1+\epsilon)b \\ \frac{1}{2} & b + \frac{a}{9} & (1+(1-c)\epsilon)b & (1+\epsilon)b \\ \frac{1}{2} + \frac{k}{12} & \frac{10}{36} + \frac{1-5a}{36}k & b + \frac{a}{9} & b \\ \frac{1}{2} + \frac{k}{4} & \frac{1}{2} + \frac{k}{12} & \frac{1}{2} & \frac{1}{2} \end{bmatrix} B(n).$$

We check the four difficult cases for monotonicity.

$$\begin{aligned} P_{22}(n) < P_{21}(n): &\qquad (1-c)\epsilon b < 0 < \frac{a}{9} \\ P_{21}(n) < P_{20}(n): &\qquad b + \frac{a}{9} = \frac{3-4a}{18} < 0 < \frac{1}{2} \\ P_{11}(n) < P_{10}(n): &\qquad \frac{10 - 18 + k - 3k - 5ak}{36} < -\frac{8+7k}{36} < 0 \\ P_{12}(n) < P_{11}(n): &\qquad \frac{6 - 8a - 10 - k + 5ak}{36} < 0 \end{aligned}$$

The last relation is responsible for the extra condition on the normal component of the A_i and B_{ij}.

LEMMA 1.3.12 *An edge between two cells with zero cut ratios is interpolated. Planar cells with zero cut ratios are covered by a planar surface.*

Proof. Step A3 applies at two types of irregularities in the mesh. A vertex irregularity originates from a vertex of the input mesh that does not have four neighbors. Here all points A_i, B_{ij}, C_i and hence all patches are coalesced into one input mesh point if the ratio is zero and hence the point is interpolated by the surface. A cell irregularity originates from a cell of the input mesh that is not quadrilateral. Here the points A_i, B_{ij}, C_i are coalesced into their respective input mesh point, say L_i and the quadratic border patches degenerate into straight lines $L_i\ M_i$ and $L_i\ M_{i-1}$ where $M_i = (L_{i+1} + L_i)/2$. Since the cubic construction averages the L_i and the L_i are coplanar, the second claim follows.

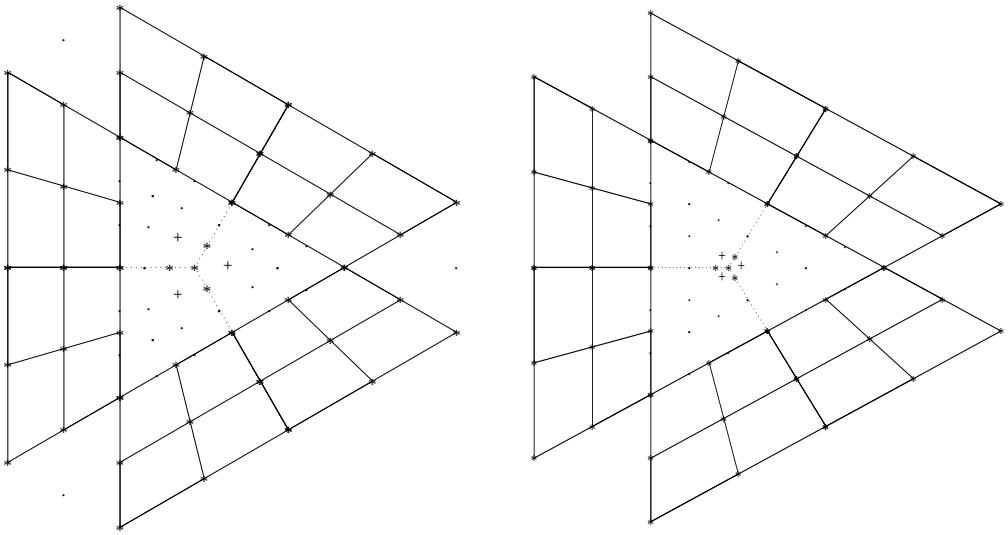

Figure 3.1: *Coefficient distribution for* $\phi = \mathrm{id} + t_1 t_2 \begin{bmatrix} a \\ a(1-t_2) \end{bmatrix}$ *and* $\phi = \mathrm{id}$.

For a similar surface construction, [18] establishes that the surface lies in the convex hull of the control mesh.

1.3.4. A remark on parametric C^1 continuity, bicubic patches and triangular mesh cells.

Choosing the extension across the boundaries of the biquadratic complex to be parametrically C^1, i.e. $\phi_{i,j}$ to be the identity, leads in general to an inconsistent system of equations for bicubics. In particular, $D_1 \psi_i^{'[1]}$ has to be at least quadratic, since $D_2 D_1 \psi_i^{'[1]}(0,0)$ is zero rather than $-2c$. This results in n additional constraints but only one of n tangent coefficients and one of n twist coefficients may be chosen freely in addition to S. Therefore, one can in general not cover an n-sided hole with bicubics that extend a biquadratic patch complex parametrically C^1 across its boundary.

An exception occurs for $n = 3$ due to the fact that three points always lie in a plane. One can then choose the boundary curves to be the quadratic $p_{i-1}(0,t) = p_i(0,t) = M_i(1-t)^2 + (C_i + C_{i+1})t(1-t) + St^2$,

$$\phi_{ij} = \mathrm{id} \quad \text{and} \quad \psi_i := \mathrm{id} + t_1(1-t_2)^2 \begin{bmatrix} 2c \\ 0 \end{bmatrix},$$

and

$$
\begin{aligned}
S &= (C_1 + C_2 + C_3)/3 \\
P_{32,i} &= (4C_i + 4C_{i+1} + C_{i-1})/9 \\
P_{22,i} &= \frac{1}{9}(7C_i + C_{i+1} + C_{i-1}) + \frac{1}{6}C_i - \frac{1}{12}\sum_{j=0}^{2}(-1)^j(B_{j,2} + B_{j+1,1}).
\end{aligned}
$$

This solution can also be applied if the surrounding patch complex is bicubic resulting in the construction of [11, Figs 4.1–3]. Figure 3.1 compares the distribution of the Bernstein-Bézier coefficients

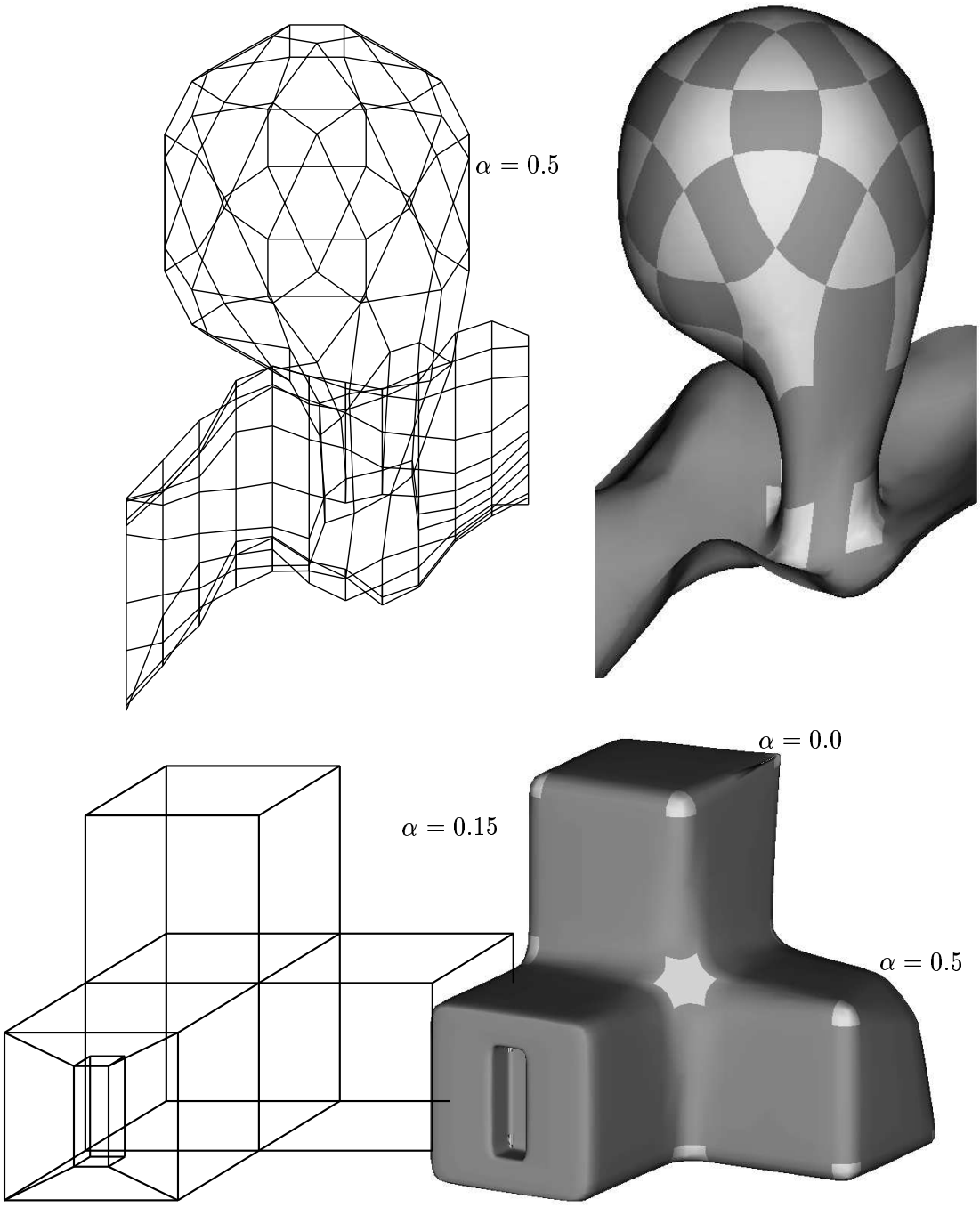

1.4. Examples

The following examples illustrate the flexibility of the algorithm with respect to the topological structure and the blend ratio. The regular mesh regions covered by a biquadratic spline complex is shaded dark. The second object uses $\alpha = 0.15$ everywhere in the first refinement except at the mesh points labeled $\alpha = 0.0$ and $\alpha = 0.5$. This illustrates a more general rule for associating blend ratios with edges to achieve locally a larger or zero blend radius. The algorithm

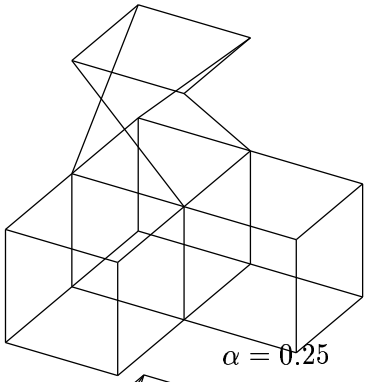

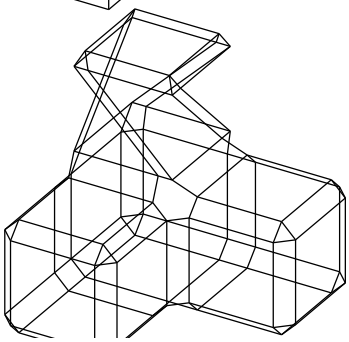

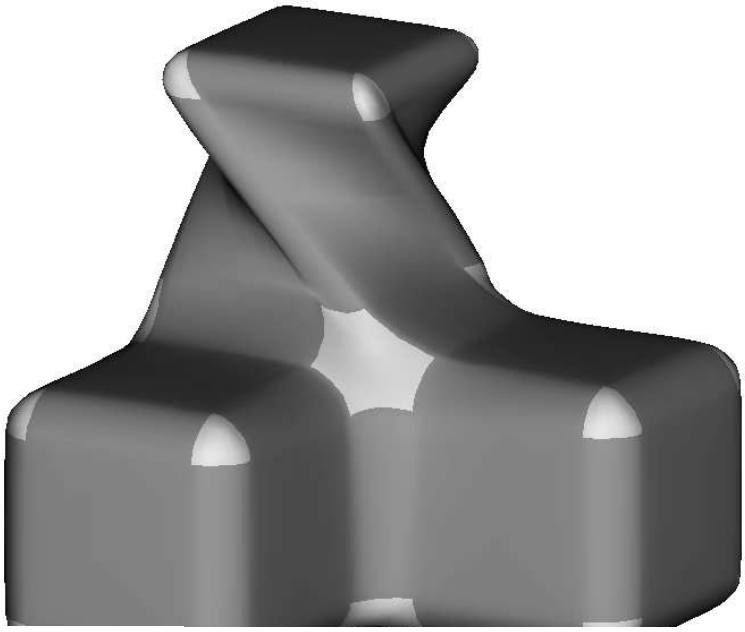

maximal absolute principal curvature

approximate reflection lines

in Section 2 uses one ratio for each cell only to simplify the exposition. The top cube of the third object is twisted to make sure that the 6-sided mesh cell at the common point of the cubes is not symmetric. The object also features irregular 3, 4 and 5-sided mesh cells. The details below show a shading by the maximum of the absolute value of the two principal curvatures. The grey values range linearly from the least curvature on the object (black) to the maximal curvature (white). High curvature concentrates in the hyperbolic twist region and along edges leading into the relatively flat six-sided region.

1.5. Conclusion

The preceding sections defined and analyzed an algorithm that generalizes the construction of biquadratic tensor-product B-spline surfaces to irregular meshes. Given a mesh of points that outlines an open or closed surface in space, the algorithm constructs a C^1 surface that closely follows the mesh. Most of the surface is parametrized by a biquadratic spline whose control points are obtained by refining the input mesh. The remaining mesh regions are parametrized by bicubic patches in Bernstein-Bézier form. The construction can be extended to rational patches and to interpolate at the vertices of the input mesh.

The algorithm combines a number of ideas and techniques from the literature with new insights. Interpreting a mesh of regular points as a control mesh for a tensor-product spline surface and, generally, refining an input mesh reflect the well-known approach of generalized subdivision. Here, however, the refinement is used for a new and different purpose. Rather than iterating to the limit, the refinement is only applied twice to give the surface its rough shape and create a new mesh with separated irregularities. Naively used, the refinement leads to a large number of polynomial pieces; in practice, one would use a hierarchical approach to evaluation and display.

The strong points of the representation are its low degree, standard tensor-product representation and the simplicity of the construction. The representation defines an interpolating spline space for modeling surfaces of arbitrary topology. The low degree of the parametrization and the construction by averaging limit the potential for introducing extraneous features when smoothing the input mesh.

References

[1] A.A. Ball, D.J.T. Storry, *A matrix approach to the analysis of recursively generated B-spline surfaces,* Computer Aided Design 18, No 8, (1986) , pp. 437–442.

[2] A.A. Ball, D.J.T. Storry, *Conditions for tangent plane continuity over recursively generated B-spline surfaces,* ACM TOG 7, No 2, (1988), pp. 83–1002.

[3] A.A. Ball, D.J.T. Storry, *Design of an n-sided surface patch from Hermite boundary data.* Computer Aided Geometric Design 6, (1989), pp. 111–120.

[4] E. Catmull, J. Clark, *Recursively generated B-spline surfaces on arbitrary topological meshes,* Computer Aided Design 10, No 6, (1978), pp. 350–355.

[5] H. Chiyokura and F. Kimura, *Design of Solids with Free-form Surfaces,* Computer Graphics, 17, No. 3, (1983), pp. 289-298.

[6] D. Doo, *A subdivision algorithm for smoothing down irregularly shaped polyhedrons,* Proceedings on interactive techniques in computer aided design, Bologna, (1978), pp. 157–165.

[7] D. Doo and M. Sabin, *Behaviour of recursive division surfaces near extraordinary points,* Computer Aided Design 10, No 6, (1978), pp. 350–355.

[8] N. Dyn, D. Levin, D. Liu, *Interpolatory convexity preserving subdivision schemes for curves and surfaces,* preprint 1992.

[9] T.N.T. Goodman, *Closed surfaces defined from biquadratic splines,* Constructive Approximation **7** 1991, 149-160.

[10] J.A. Gregory, *Smooth parametric surfaces and n-sided patches,* Computation

of curves and Surfaces, W. Dahmen, M. Gasca and C.A. Micchelli, eds., Kluwer Academic Publishers, Dordrecht, 1990, pp. 457–498.

[11] J.A. Gregory, J. Zhou(1990), *Filling polygonal holes with bicubic patches,* TR-05-91, Brunel University,Uxbridge, UB8 3PH, England, March 1991.

[12] J. M. Hahn, *Filling polygonal holes with rectangular patches,* Theory and Practice of geometric modeling, W. Straßer and H.-P. Seidel eds., Springer 1989.

[13] K. Höllig, H. Mögerle, *G-splines,* Computer Aided Geometric Design **7**, (1989), pp. 197–207.

[14] C. Loop *Smooth subdivision surfaces based on triangles,* Master's thesis, (1987), University of Utah.

[15] C. Loop *A G^1 triangular spline surface of arbitrary topology,* manuscript, Dept. of CS and Eng., (1990), University of Washington, April 1990.

[16] C. Loop, T. DeRose, *Generalized B-spline surfaces of arbitrary topology,* Proceedings of Siggraph '90.

[17] H. Mögerle, *G-splines höherer Ordnung*, thesis, Math Inst A, University of Stuttgart, Germany, (1992).

[18] J. Peters, C^1 free-form surface splines *SIAM Numer. Anal.* **x** 199x.

[19] M. Sabin, *Non-rectangular surface patches suitable for inclusion in a B-spline surface,* in P. ten Hagen (ed.), Proceedings of Eurographics '83, North Holland, 1983, pp. 57–69.

[20] R.F. Sarraga, *G^1 Interpolation of Generally Unrestricted Cubic Bézier curves,* Computer Aided Geometric Design 4(1-2), (1987), pp. 23–40,1987.

[21] J.J. van Wijk, *Bicubic patches for approximating non-rectangular control-point meshes,* Computer Aided Geometric Design 3, No 1, (1984), pp. 1–13.